

PREPARATION AND CHARACTERIZATION OF VISIBLE-LIGHT-DRIVEN Ce-DOPED CdS NANOWIRES FOR PHOTODEGRADATION OF RHODAMINE B

A. PHURUANGRAT^{a,*}, T. SAKHON^b, T. THONGTEM^{c,d}, S. THONGTEM^{c,e}

^a*Division of Physical Science, Faculty of Science, Prince of Songkla University, Hat Yai, Songkhla 90112, Thailand*

^b*Electron Microscopy Research and Service Center, Faculty of Science, Chiang Mai University, Chiang Mai 50200, Thailand*

^c*Materials Science Research Center, Faculty of Science, Chiang Mai University, Chiang Mai 50200, Thailand*

^d*Department of Chemistry, Faculty of Science, Chiang Mai University, Chiang Mai 50200, Thailand*

^e*Department of Physics and Materials Science, Faculty of Science, Chiang Mai University, Chiang Mai 50200, Thailand*

Visible-light-driven Ce-doped CdS nanowires were synthesized by a solvothermal method. Phase and morphology of Ce-doped CdS nanowires were investigated by XRD and SEM analyses. The analytical results certified that both CdS and Ce-doped CdS samples were uniform pure phase of hexagonal CdS nanowires. The photocatalytic activities of CdS and Ce-doped CdS nanowires were investigated through the photodegradation of rhodamine B (RhB) under visible light irradiation. The 3% Ce-doped CdS nanowires have the highest photocatalytic efficiency of 95.75% within 120 min and are the promising material used for wastewater treatment.

(Received November 25, 2020; Accepted February 13, 2021)

Keywords: Ce-doped CdS nanowires; Photocatalysis; Spectroscopy

1. Introduction

In recent years, water pollution caused by organic pollutants from different industries, such as paper, textile, pigment, cosmetic, food and drug manufacturing has become a global issue due to its diverse effects on environment and living organisms [1-4]. Several conventional treatment methods of organic pollutants from wastewater including biodegradation, absorption, membrane filtration, flocculation-coagulation and ozonation have a common drawback because they are unable to completely remove dyes from wastewater, including the cause of secondary pollution and expensive treatment process [1, 2, 4, 5]. Thus, a visible light driven photocatalyst as green technology has been focused in the degradation of environmental pollutants under visible light by active radicals because visible light is available in the solar spectrum and is abundant (~43%) much more than UV light (~4%) [2, 5-7].

Currently, cadmium sulfide (CdS) as II-VI type semiconductor shows the outstanding performance as a visible light driven photocatalyst in the field of environmental treatment due to its effective direct band gap of 2.42 eV, low cost, photostability and appropriate conduction band potential [1, 2, 8-10]. It is widely used in many applications including physicochemical, photoluminescence and potential application in many fields such as photovoltaic material, gas sensors, photo detectors, light-emitting diodes, window materials, solar cells, optoelectronic and piezoelectric devices [1, 11, 12]. Nevertheless, the photocatalytic performance of CdS is limited by its rapid recombination of photo-generated charge carriers in photocatalytic reaction under visible light irradiation and photo-corrosion in air [2, 8, 9]. Thus, rare earth metal ions such as La, Ce, Yb, Tb, Pr and Sm are doped in the semiconductor photocatalyst which can lead to improve the

* Corresponding author: phuruangrat@hotmail.com

photocatalytic performance by inhibiting the combination of photo-excited electron and photo-induced hole pairs and to enlarge the range of light absorption of the semiconductor [5, 13-15].

In this work, the visible-light-driven photocatalytic Ce-doped CdS nanowires were synthesized by solvothermal method. Phase and morphology of CdS and Ce-doped CdS nanomaterials were studied. The photocatalytic activities of CdS and Ce-doped CdS nanomaterials were investigated by photodegradation of rhodamine B (RhB) under visible light irradiation. The results revealed that Ce dopant can play the role in improving the photocatalytic activity of CdS under visible light irradiation.

2. Experimental procedure

To synthesize CdS doped with different contents of Ce, 0.001 mole $\text{Cd}(\text{NO}_3)_2 \cdot 4\text{H}_2\text{O}$ and 0–3 % $\text{Ce}(\text{NO}_3)_3 \cdot 6\text{H}_2\text{O}$ by mole were dissolved in 50 ml ethylenediamine solutions. Subsequently, each 50 ml of 0.001 mole NH_2CSNH_2 in ethylenediamine solution was added to the above solutions which were continuously stirred for 30 min. They were put in 200 ml of home-made stainless steel autoclaves and heated in an electric oven at 200 °C for 24 h. The light yellow-orange precipitates were filtered, washed with distilled water several times and absolute ethanol, and dried at 60 °C for 24 h. The crystalline phase and morphology investigation of pure CdS and Ce-doped CdS samples were characterized by an X-ray diffractometer (XRD, Philips X'Pert MPD) operating at 45 kV 35 mA and using Cu-K_α line in the 2θ of 10°–60° range and a field emission scanning electron microscope (FE-SEM, JEOL JSM-6335F) operating at 35 kV.

Photocatalytic activity was evaluated through the degradation of rhodamine B (RhB) solution using a xenon lamp as a visible light source with a 420 nm cut-off wavelength filter. The 0.2 g photocatalyst was added to 1×10^{-5} M of 200 ml RhB solutions which were continuously stirred in the dark for 30 min to form homogeneous solutions. Under visible light irradiation, ~5 ml solution was withdrawn from the tested solution every 30 min and centrifuged to remove the residual photocatalyst. The content of RhB solution was measured by a PerkinElmer Lambda 25 UV–visible spectrophotometer at λ_{max} of 554 nm. The degradation efficiency was calculated by the below equation.

$$\text{Decolorization efficiency (\%)} = \frac{C_0 - C_t}{C_0} \times 100 \quad (1)$$

C_0 is the initial concentration of RhB in dark condition and C_t is the concentration of RhB after visible light irradiation within the elapsed time (t).

3. Results and discussion

Fig. 1 shows XRD patterns of the CdS nanostructure with different concentration of Ce dopant. All diffraction peaks of pure CdS sample without Ce doping correspond with the wurtzite hexagonal CdS structure as compared to the reference JCPDS No. 77-2306 [16]. Other characteristic diffraction peaks of impurities were not detected. Thus, the CdS sample is high purified phase. Furthermore, XRD patterns of Ce-doped CdS with different concentration of Ce dopant were similar to that of the hexagonal CdS structure, indicating that the Ce dopant did not play the role in the phase of hexagonal CdS structure. It suggests that Ce^{3+} ions were successfully substituted for Cd^{2+} ions of CdS lattice. The XRD patterns of Ce-doped CdS clearly showed that the diffraction peaks were shifted as compared to those of the pure CdS sample. This leads to an expansion of unit cell and the size effect. Clearly, the positions of main diffraction peaks of Ce-doped CdS were shifted to higher angle because the ionic radius of Ce^{3+} ion (1.14 Å [17-20]) is larger than that of Cd^{2+} ion (1.03 Å [21, 22]). The unit cell parameters are $a = 4.1388$ Å and $c = 6.7125$ Å for pure CdS sample and $a = 6.7125$ Å and $c = 6.6666$ Å for the 3% Ce-doped CdS

sample. Thus, the unit cell volume of pure CdS sample is slightly larger than that of 3% Ce-doped CdS nanostructure due to the introduction of cerium ions into CdS lattice [13-15].

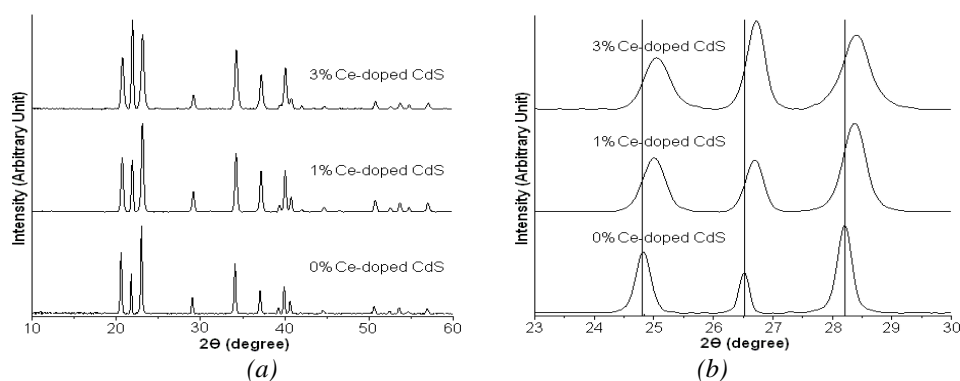


Fig. 1. X-ray diffraction patterns of 0–3% Ce-doped CdS samples synthesized by solvothermal method at 2θ range of (a) $10\text{--}60^\circ$ and (b) $23\text{--}30^\circ$.

The morphologies of CdS and 3% Ce-doped CdS samples were observed by SEM as the results shown in Fig. 2. The low magnification SEM image of CdS without Ce dopant presents that the sample is composed of uniform nanowires with length in the range of 2–3 μm . The high magnification SEM image of CdS without Ce dopant demonstrates the presence of CdS nanowires with 20–30 nm diameter and smooth surface grew along the [001] direction. Upon doping with Ce, the doped sample shows the same morphology as the pure CdS sample. The diameter and length of 3% Cd-doped CdS nanowires are 30–50 nm and 2–4 μm , respectively. No other morphologies of the 3% Cd-doped CdS were detected, indicating that the 3% Cd-doped CdS sample has highly uniform morphology.

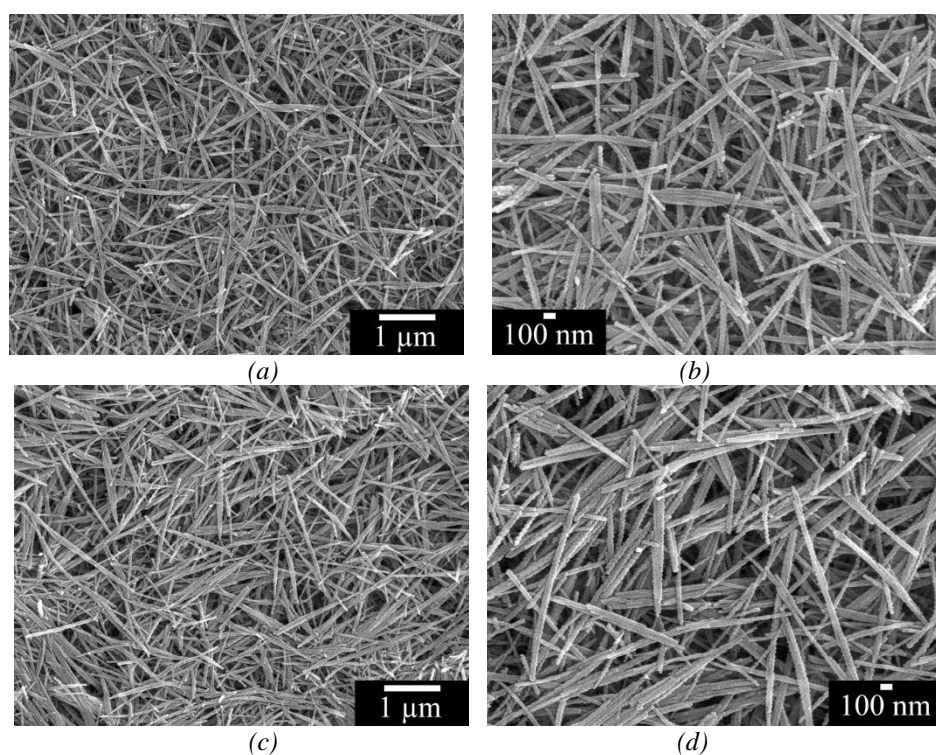


Fig. 2. SEM images of (a and b) CdS and (c and d) 3% Ce-doped CdS nanowires synthesized by solvothermal method at low and high magnifications.

The photocatalytic activities of CdS with different concentration of Ce dopant were studied through the degradation of RhB under visible light irradiation within 120 min. The absorption spectra of the RhB dye solution exposed to visible light for different time periods in the presence of 3% Ce-doped CdS nanowires are shown in Fig. 3. The maximum absorption peak of RhB at 554 nm was rapidly decreased with the increase of visible light irradiation time. It almost disappeared after 120 min of irradiation and accompanied by the blue shift process. Thus, the RhB was degraded by a series of N-deethylated intermediates during photocatalysis [23-25].

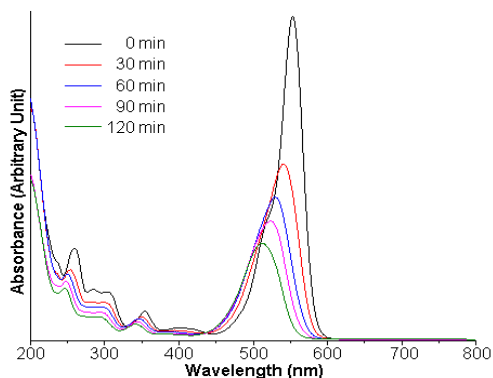


Fig. 3. UV-visible absorption of RhB in the solution containing 3% Ce-doped CdS nanowires under visible light irradiation within 120 min.

Fig. 4a shows the photocatalytic efficiencies of CdS containing different contents of Ce dopant. The degradation efficiency of CdS nanowires under visible light irradiation within 120 min is 92.02% while those of 1%Ce-doped CdS, 2%Ce-doped CdS and 3%Ce-doped CdS were increased to 93.52%, 94.76% and 95.75%, respectively. Clearly, the Ce dopant played the role in improving the photocatalytic performance of CdS because Ce acted as an electron acceptor and inhibited the recombination of electrons and holes during photocatalytic reaction [13, 15]. The kinetics behavior for photodegradation of RhB over CdS and Ce-doped CdS was further investigated and the pseudo-first-order reaction model is shown in Fig. 4b.

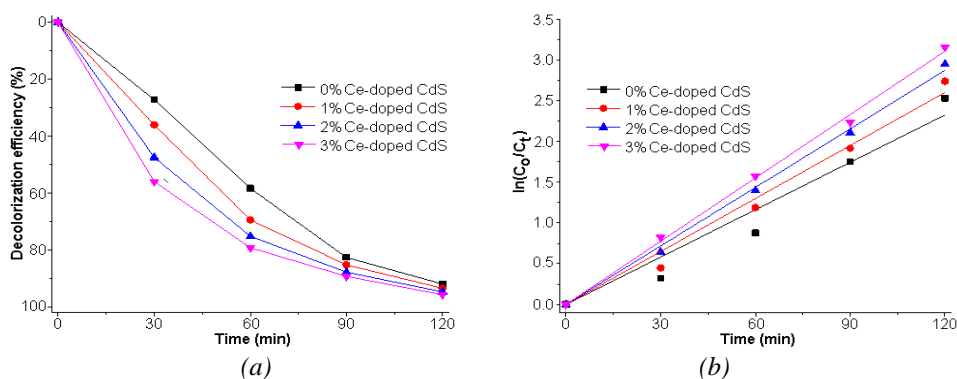


Fig. 4. (a) Decolorization efficiency and (b) kinetics rate reaction for photodegradation of RhB over 0, 1, 2 and 3% Ce-doped CdS nanowires during visible light illumination within 120 min.

The plot shows the linear correlation with the time of photocatalytic reaction ($R^2 > 0.98$). The results indicate that the photodegradation of RhB over CdS and Ce-doped CdS is in accordance with the pseudo-first-order reaction [15, 23, 25-27]. The reaction rate constants for photodegradation of RhB for 0%, 1%, 2% and 3% Ce-doped CdS nanowires are 0.0192, 0.0218, 0.0239 and 0.0261 min^{-1} , respectively. Obviously, the rate constant of 3% Ce-doped CdS nanowires is 1.36 times that of the as-synthesized CdS nanowires. The photocatalytic activity of

CdS is greatly improved by introducing an appropriate amount of Ce dopant. In addition, the stability and recyclability of 3% Ce-doped CdS nanowires were investigated through RhB degradation for five recycles. At the end of each reaction cycle, the photocatalyst was collected and dried for further reuse of the next cycle as the results shown in Fig 5. At the end of cycle five, the photodegradation of RhB was 90.35%. Clearly, 3% Ce-doped CdS nanowires remain as the photocatalyst for wastewater treatment under visible radiation.

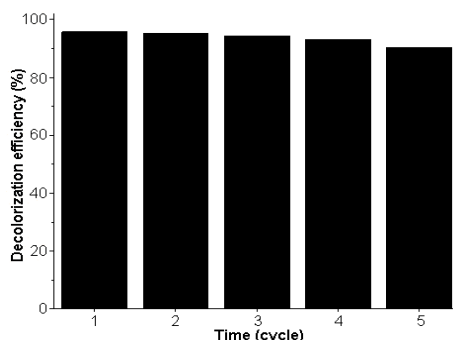


Fig. 5. The repeated photocatalytic test of reused 3 % Ce-doped CdS nanowires for RhB degradation under visible light irradiation.

The primary active species of RhB degradation were studied using isopropanol (IPA), benzoquinone (BQ) and triethanolamine (TEOA) as the scavengers for $\cdot\text{OH}$, $\cdot\text{O}_2^-$ and h^+ as the results shown in Fig. 6 [28-31]. Upon the addition of IPA and BQ, the photodegradation of RhB was greatly restrained because IPA and BQ trapped the $\cdot\text{OH}$ and $\cdot\text{O}_2^-$ radicals. The results indicated that $\cdot\text{OH}$ and $\cdot\text{O}_2^-$ are the main active species for RhB degradation over 3% Ce-doped CdS nanowires. In case of TEOA adding, the photodegradation of RhB was slightly decreased. Thus, $\cdot\text{OH}$ and $\cdot\text{O}_2^-$ radicals are the main active species for the photodegradation of RhB over 3% Ce-doped CdS nanowires under visible light irradiation.

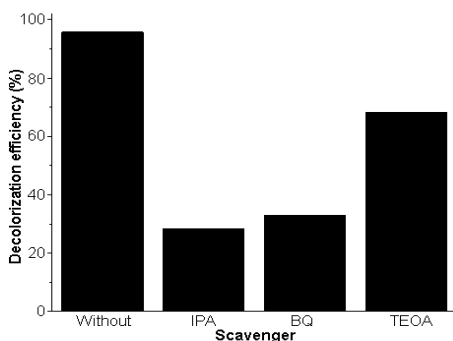


Fig. 6. Comparison of photocatalytic activities of 3 % Ce-doped CdS nanowires containing in RhB solutions with and without different scavengers.

4. Conclusions

In summary, Ce-doped CdS nanowires were synthesized by solvothermal method. The XRD and SEM analyses indicated the pure hexagonal phase of Ce-doped CdS nanowires with growth direction in [001]. The photodegradation of RhB over 3% Ce-doped CdS nanowires was the highest of 95.75% within 120 min under visible light irradiation because Ce as an electron acceptor played the role in inhibiting the recombination of electrons and holes during photocatalytic reaction. The 3% Ce-doped CdS nanowires were high stable and reusable for photocatalytic reaction within five recycled test. Thus, Cd-doped CdS nanowires are a promising visible-light-driven photocatalyst for wastewater treatment.

Acknowledgement

We wish to thank Center of Excellence in Materials Science and Technology, Chiang Mai University, for financial support under the administration of Materials Science Research Center, Faculty of Science, Chiang Mai University, Thailand.

References

- [1] U. A. Khan, J. Liu, J. Pan, H. Ma, S. Zuo, Y. Yu, A. Ahmad, B. Li, *Mater. Sci. in Semicond. Process.* **83**, 201 (2018).
- [2] A. Arabzadeh, A. Salimi, *J. Colloid Interf. Sci.* **479**, 43 (2016).
- [3] Q. Wang, J. Li, Y. Bai, X. Lu, Y. Ding, S. Yin, H. Huang, H. Ma, F. Wang, B. Su, *J. Photochem. Photobiol. B* **126**, 47 (2013).
- [4] A. Ahmad, S. H. Mohd-Setapar, C. S. Chuong, A. Khattoon, W. A. Wani, R. Kumard, M. Rafatullah, *RSC Adv.* **5**, 30801 (2015).
- [5] P. Venkataswamy, M. Sudheera, K. Vaishnavi, K. Ramaswamy, G. Ravi, M. Vithal, *J. Electron. Mater.* **49**, 2358 (2020).
- [6] R. Maity, M. S. Sheikh, A. Dutta, T. P. Sinha, *J. Electron. Mater.* **48**, 4856 (2019).
- [7] A. Phuruangrat, S. Thongtem, T. Thongtem, *J. Electron. Mater.* **48**, 8031 (2019).
- [8] P. Wang, T. Wu, Y. Ao, C. Wang, *Renew. Energy* **131**, 180 (2019).
- [9] M. M. Kandy, V. G. Gaikar, *Renew. Energy* **139**, 901 (2019).
- [10] X. Zhao, X. Wang, Z. Sun, Z. Li, D. Sun, *Optik* **208**, 164543 (2020).
- [11] Z. Suo, J. Dai, S. Gao, H. Gao, *Results Phys.* **17**, 103058 (2020).
- [12] A. Nazir, A. Toma, N. A. Shah, S. Panaro, S. Butt, R. R. Sagar, W. Raja, K. Rasool, A. Maqsood, *J. Alloy. Compd.* **609**, 40 (2014).
- [13] H. Shi, T. Zhang, T. An, B. Li, X. Wang, *J. Colloid Interf. Sci.* **380**, 121 (2012).
- [14] C. He, X. Li, X. Chen, S. Ma, X. Yan, Y. Zhang, S. Zuo, C. Yao, *Appl. Clay Sci.* **184**, 105398 (2020).
- [15] M. Nithya, U. Sathya, Keerthi, *Optik* **193**, 163007 (2019).
- [16] Powder Diffract. File, JCPDS Internat. Centre Diffract. Data, PA 19073–3273, U.S.A. (2001).
- [17] M. Meddouri, L. Hammiche, O. Slimi, D. Djouadi, A. Chelouche, *Mater. Sci.-Poland* **34**, 659016).
- [18] I. Ahemen, F.B. Dejene, *J. Mater. Sci.* **29**, 2140 (2018).
- [19] W. Lee, S.Y. Chen, E. Tseng, A. Gloter, C. L. Chen, *J. Phys. Chem. C* **120**, 14874 (2016).
- [20] J. Dukić, S. Bošković, B. Matovic, *Ceram. Int.* **35**, 787 (2009).
- [21] S. L. Galagali, R. A. Patil, R. B. Adaki, C. S. Hiremath, S. N. Mathad, A. S. Pujar, R. B. Pujar, *Songklanakarin J. Sci. Technol.* **41**, 992 (2019).
- [22] P. Castaldi, M. Silveti, L. Santona, S. Enzo, P. Melis, *Clays Clay Miner.* **56**, 461 (2008).
- [23] H. Guo, C. G. Niu, X. J. Wen, L. Zhang, C. Liang, X. G. Zhang, D. L. Guan, N. Tang, G. M. Zeng, *J. Colloid Interf. Sci.* **513**, 852 (2018).
- [24] M. R. Chandra, T. S. Rao, H. S. Kim, S. V. N. Pammi, N. Prabhakar Rao, I. M. Raju, *J. Asian Ceram. Soc.* **5**, 436 (2017).
- [25] H. Yin, M. Zhang, J. Yao, Y. Luo, P. Li, X. Liu, S. Chen, *Mater. Sci. Semicond. Process.* **105**, 104688 (2020).
- [26] A. Phuruangrat, B. Kuntalue, T. Thongtem, S. Thongtem, *Chalcogenide Lett.* **16**, 149 (2019).
- [27] A. Phuruangrat, K. Karthik, B. Kuntalue, P. Dumrongrojthanath, S. Thongtem, T. Thongtem, *Chalcogenide Lett.* **16**, 387 (2019).
- [28] H. Liang, S. Liu, H. Zhang, X. Wang, J. Wang, *RSC Adv.* **8**, 13625 (2018).
- [29] G. Wu, L. Xiao, W. Gu, W. Shi, D. Jiang, C. Liu, *RSC Adv.* **6**, 19878 (2016).
- [30] R. Lei, H. Ni, R. Chen, H. Gu, B. Zhang, W. Zhan, *J. Nanopart. Res.* **19**, 378 (2017).
- [31] L. Zong, P. Cui, F. Qin, K. Zhao, Z. Wang, R. Yu, *Mater. Res. Bull.* **86**, 44 (2017).